

2-15-2017

## Mechanisms of modulation of brain microvascular endothelial cells function by thrombin.

Eugen Brailoiu  
*Temple University School of Medicine*

Megan M. Shipsky  
*Thomas Jefferson University*

Guang Yan  
*Thomas Jefferson University*

Mary E. Abood  
*Temple University School of Medicine*

G. Cristina Brailoiu  
*Thomas Jefferson University*  
Follow this and additional works at: <https://jdc.jefferson.edu/pharmacyfp>

 Part of the [Pharmacy and Pharmaceutical Sciences Commons](#)

[Let us know how access to this document benefits you](#)

---

### Recommended Citation

Brailoiu, Eugen; Shipsky, Megan M.; Yan, Guang; Abood, Mary E.; and Brailoiu, G. Cristina, "Mechanisms of modulation of brain microvascular endothelial cells function by thrombin." (2017). *College of Pharmacy Faculty Papers*. Paper 33.  
<https://jdc.jefferson.edu/pharmacyfp/33>

This Article is brought to you for free and open access by the Jefferson Digital Commons. The Jefferson Digital Commons is a service of Thomas Jefferson University's [Center for Teaching and Learning \(CTL\)](#). The Commons is a showcase for Jefferson books and journals, peer-reviewed scholarly publications, unique historical collections from the University archives, and teaching tools. The Jefferson Digital Commons allows researchers and interested readers anywhere in the world to learn about and keep up to date with Jefferson scholarship. This article has been accepted for inclusion in College of Pharmacy Faculty Papers by an authorized administrator of the Jefferson Digital Commons. For more information, please contact: [JeffersonDigitalCommons@jefferson.edu](mailto:JeffersonDigitalCommons@jefferson.edu).



Published in final edited form as:

*Brain Res.* 2017 February 15; 1657: 167–175. doi:10.1016/j.brainres.2016.12.011.

## Mechanisms of modulation of brain microvascular endothelial cells function by thrombin

Eugen Brailoiu<sup>1</sup>, Megan M. Shipy<sup>2</sup>, Guang Yan<sup>2</sup>, Mary E Abood<sup>1</sup>, and G. Cristina Brailoiu<sup>2,\*</sup>

<sup>1</sup>Center for Substance Abuse Research, Temple University School of Medicine, Philadelphia, PA 19140

<sup>2</sup>Department of Pharmaceutical Sciences, Thomas Jefferson University, Jefferson College of Pharmacy, Philadelphia, PA 19107

### Abstract

Brain microvascular endothelial cells are a critical component of the blood-brain barrier. They form a tight monolayer which is essential for maintaining the brain homeostasis. Blood-derived proteases such as thrombin may enter the brain during pathological conditions like trauma, stroke, and inflammation and further disrupts the permeability of the blood-brain barrier, via incompletely characterized mechanisms. We examined the underlying mechanisms evoked by thrombin in rat brain microvascular endothelial cells (RBMVEC). Our results indicate that thrombin, acting on protease-activated receptor 1 (PAR1) increases cytosolic  $\text{Ca}^{2+}$  concentration in RBMVEC via  $\text{Ca}^{2+}$  release from endoplasmic reticulum through inositol 1,4,5-trisphosphate receptors and  $\text{Ca}^{2+}$  influx from extracellular space. Thrombin increases nitric oxide production; the effect is abolished by inhibition of the nitric oxide synthase or by antagonism of PAR1 receptors. In addition, thrombin increases mitochondrial and cytosolic reactive oxygen species production via PAR1-dependent mechanisms. Immunocytochemistry studies indicate that thrombin increases F-actin stress fibers, and disrupts the tight junctions. Thrombin increased the RBMVEC permeability assessed by a fluorescent flux assay. Taken together, our results indicate multiple mechanisms by which thrombin modulates the function of RBMVEC and may contribute to the blood-brain barrier dysfunction.

### Keywords

blood-brain barrier; calcium signaling; cerebral microvasculature; protease-activated receptor 1

### 1. Introduction

Endothelial cells of brain capillaries are an essential component of the blood-brain barrier; they contribute to brain homeostasis by forming a tight layer with reduced permeability (Abbott et al., 2010; Cardoso et al., 2010). The activity of brain microvascular endothelial

\* Address correspondence to G.C. Brailoiu, M.D., Department of Pharmaceutical Sciences, Thomas Jefferson University, Jefferson College of Pharmacy, 901 Walnut St, Suite 901, Philadelphia, PA 19107, Phone: 215-503-7468; Gabriela.Brailoiu@jefferson.edu.

**Conflict of interest statement** All authors declare that there are no conflicts of interest.

cells is modulated by G protein-coupled receptors agonists such as bradykinin, histamine, glutamate and thrombin through  $\text{Ca}^{2+}$ -dependent mechanisms (Brown et al., 2008; De Bock et al., 2013; Kuhlmann et al., 2008; Li et al., 1999).

Thrombin is a blood-derived protease whose primary role is in coagulation and wound healing (Siller-Matula et al., 2011). During pathological conditions such as head trauma, stroke or inflammation, when the integrity of the blood-brain barrier is compromised, thrombin, and other blood-derived proteases may enter the brain and further impair the permeability of the blood-brain barrier (Cirino et al., 2000; Gingrich and Traynelis, 2000; Kuhlmann et al., 2008). In addition, brain endothelial cells can synthesize thrombin in neurodegenerative disorders like Alzheimer's disease (Yin et al., 2010).

Thrombin has been reported to increase the permeability of endothelial cells from various vascular beds, including brain microvessels (Arce et al., 2008; Bartha et al., 2000; Kim et al., 2004; Siller-Matula et al., 2011); however, the mechanisms are incompletely understood. The effects of thrombin are largely mediated by protease-activated receptor 1 (PAR1), the first identified G protein-coupled receptor that is activated by proteolysis (Rasmussen et al., 1991; Vu et al., 1991). Three additional proteinase-activated receptors (PARs) have been identified; PAR3 and PAR4 can be also activated by thrombin, while PAR2 is activated by trypsin (Alexander et al., 2015; Hollenberg and Compton, 2002).

Rat and human brain microvascular endothelial cells express thrombin receptors PAR1, PAR3 and PAR4 (Bartha et al., 2000; Kim et al., 2004; Vajda et al., 2008). Common signaling mechanisms downstream of thrombin-PARs interaction include activation of  $\text{G}_{q/11}$  proteins followed by mobilization of intracellular  $\text{Ca}^{2+}$  (Alexander et al., 2015; Hollenberg and Compton, 2002).

The endothelial cytosolic  $\text{Ca}^{2+}$  concentration,  $[\text{Ca}^{2+}]_i$ , is an essential determinant of paracellular permeability; an increase in  $[\text{Ca}^{2+}]_i$  produces barrier dysfunction, by modulating the arrangement of junctional and cytoskeletal proteins (De Bock et al., 2013; Tiruppathi et al., 2002). Previous studies indicate that cytosolic  $\text{Ca}^{2+}$  plays a central role in the barrier disruption produced by thrombin (Kim et al., 2004; Sandoval et al., 2001). However, different  $\text{Ca}^{2+}$ -dependent mechanisms are evoked by thrombin in different vascular beds (Arce et al., 2008; Sandoval et al., 2001). The current study examined the effects of thrombin on cytosolic  $\text{Ca}^{2+}$  concentration, nitric oxide, mitochondrial and cytosolic reactive oxygen species (ROS) production, cytoskeleton and tight junctions, and permeability, in rat brain microvascular endothelial cells.

## 2. Results

### 2.1. Thrombin increases cytosolic $\text{Ca}^{2+}$ concentration, $[\text{Ca}^{2+}]_i$ , in RBMVEC

In Fura-2 AM-loaded RBMVEC, thrombin (0.5 u/ml) increased the F340/F380 fluorescence ratio; representative examples of changes in ratio are shown in Fig. 1A. Pretreatment with the non-peptide PAR-1 antagonist, FR-171113 (1  $\mu\text{M}$ , 15 min), prevented the thrombin-induced increase in F340/F380 ratio (Fig. 1A). When the fluorescence ratio was converted to cytosolic  $\text{Ca}^{2+}$  concentration,  $[\text{Ca}^{2+}]_i$ , thrombin (0.1 u/ml, 0.5 u/ml and 1 u/ml) produced a

fast and transient increase in  $[Ca^{2+}]_i$  in a dose-dependent manner. Examples of increases in  $[Ca^{2+}]_i$  are shown in Fig. 1B, and the comparison of the amplitude of  $[Ca^{2+}]_i$  increase produced by each concentration of thrombin tested and by thrombin (0.5 u/ml) in the presence of FR-171113 (1  $\mu$ M) is shown in Fig. 1C. Thrombin (0.1u/ml, 0.5 u/ml and 1 u/ml) increased  $[Ca^{2+}]_i$  by  $52 \pm 1.3$  nM (n = 43),  $412 \pm 3.8$  nM (n = 49), and  $617 \pm 4.2$  nM (n = 51); this effect was abolished by FR-171113 (n = 42).

## 2.2. Thrombin releases $Ca^{2+}$ from endoplasmic reticulum

In  $Ca^{2+}$ -free HBSS, thrombin (0.5 u/ml) produced an increase in  $[Ca^{2+}]_i$  of lower amplitude than in  $Ca^{2+}$ -containing HBSS;  $[Ca^{2+}]_i = 239 \pm 2.7$  nM (n = 47), as compared to  $412 \pm 3.8$  nM (Fig 2). When lysosomal  $Ca^{2+}$  stores were disrupted with bafilomycin A1 (1  $\mu$ M, 1 h), a blocker of lysosomal ATPase (Bowman et al., 1988), thrombin (0.5 u/ml) increased  $[Ca^{2+}]_i$  by  $227 \pm 3.4$  nM (n = 52), which was not significantly different from the response in the absence of bafilomycin A1. Blockade of ryanodine receptors with ryanodine (1  $\mu$ M, 1 h) reduced the response to thrombin ( $[Ca^{2+}]_i = 134 \pm 2.6$  nM) (n = 43), while blockade of while inositol 1,4,5 trisphosphate ( $IP_3$ ) receptors with xestospongine C (10  $\mu$ M, 15 min) and 2-APB (100  $\mu$ M, 15 min) abolished the response to thrombin;  $[Ca^{2+}]_i = 11 \pm 1.4$  nM (n = 36) (Fig. 2).

## 2.3. Thrombin increases NO production in RBMVEC

In cells loaded with DAF-FM diacetate, a dye used to assess the NO levels (Kojima et al., 1998), thrombin (0.5 u/ml) increased the DAF-FM fluorescence ratio by about 18% ( $DAF-FM = 0.18 \pm 0.019$ ) (n = 31). The response to thrombin was markedly reduced in cells pretreated with the NO synthase inhibitor, NG-nitro-L-arginine methyl ester (L-NAME, 100  $\mu$ M), ( $DAF-FM = 0.05 \pm 0.007$ ) (n = 37) or with the PAR-1 antagonist, FR-171113 (1  $\mu$ M) ( $DAF-FM = 0.03 \pm 0.008$ ; n = 36) (Fig. 3). FR-171113 (1  $\mu$ M) alone did not produce a statistically significant increase in the DAF-FM fluorescence ratio, as compared to control (Fig. 3).

## 2.4. Thrombin increases mitochondrial superoxide in RBMEC

The effect of thrombin on mitochondrial superoxide was assessed in RBMVEC loaded with MitoSOX Red, a dye that selectively targets mitochondria. Thrombin (0.5 u/ml) increased MitoSOX Red fluorescence by 47% ( $MitoSOX\ Red = 0.47 \pm 0.016$ ; n = 37); this effect was prevented by the PAR-1 antagonist, FR-171113 (1  $\mu$ M) ( $MitoSOX\ Red = 0.06 \pm 0.041$ ; n = 39) (Fig. 4). FR-171113 (1  $\mu$ M) alone did not significantly affect the MitoSOX Red fluorescence (Fig. 4).

## 2.5. Thrombin increases cytosolic ROS in RBMVEC

In RBMVEC loaded with CM- $H_2$ -DCFDA, a dye used for the assessment of cytosolic ROS, thrombin (0.5 u/ml) produced an increase in fluorescence by about 80% ( $CM-H_2-DCFDA = 0.838 \pm 0.018$ ) (n = 41) suggesting an increase in cytosolic ROS production. The response to thrombin was abolished by the PAR-1 antagonist, FR-171113, ( $CM-H_2-DCFDA = 0.102 \pm 0.063$ ; n = 37) (Fig. 5); FR-171113 (1  $\mu$ M) did not have a significant effect by itself (Fig. 5).

## 2.6. Thrombin induces cytoskeletal changes

Immunocytochemistry studies examined the distribution of F-actin cytoskeleton and of ZO-1, a component of tight junctions (Abbott et al., 2010) before and after treatment with thrombin (0.5 u/ml), or thrombin in cells pretreated with the PAR1 antagonist, FR-171113 (1  $\mu$ M). Treatment with thrombin increased the F-actin stress fiber formation, and disrupted the tight junctions, as seen by the reduction of peripheral ZO-1 staining. In addition, thrombin promoted the intercellular gap formation (Fig. 6).

## 2.7. Thrombin increases RBMVEC permeability

Permeability of RBMVEC monolayer was assessed by FITC-dextran flux assay, as described (Monaghan-Benson and Wittchen, 2011). Confluent monolayers grown on PET inserts with 1  $\mu$ m pores were treated with thrombin (0.5 u/ml), or thrombin (0.5 u/ml) and PAR1 antagonist (1  $\mu$ M) and the fluorescence of the lower chamber was assessed at different time points (15 min, 30 min, 45 min, 1 h, 2h) using a plate reader. The fluorescence was significantly higher in samples from the lower chamber of thrombin-treated inserts; as compared with control samples, between 45 min and 2 hours ( $P < 0.05$ ) (Fig. 6B), indicating an increase in permeability.

## 3. Discussion

Thrombin, a serine protease produced by proteolysis of prothrombin at sites of vascular injury, has critical roles in coagulation and hemostasis. In addition, thrombin has pleiotropic effects in inflammation, proliferation, angiogenesis and vascular permeability (Siller-Matula et al., 2011). Thrombin increases permeability in various vascular beds such as pulmonary microvascular endothelial cells (Arce et al., 2008), rat and mouse cerebral microvascular endothelial cells (Bartha et al., 2000; Hawkins et al., 2015; Hun Lee et al., 2015; Wang et al., 2016), and human umbilical vein cells (Sandoval et al., 2001) by activating of proteinase-activated receptors (PARs).

In the present study, we examined the effects of thrombin on rat brain microvascular endothelial cells (RBMVEC), a key component of the blood-brain barrier. Since activation of PARs by thrombin has been reported to induce Gq/11-mediated signaling (Alexander et al., 2015; Hollenberg and Compton, 2002), and  $\text{Ca}^{2+}$  is an important second messenger involved in the regulation of barrier function (De Bock et al., 2013), we first investigated the effect of thrombin on cytosolic  $\text{Ca}^{2+}$  concentration,  $[\text{Ca}^{2+}]_i$ .

In RBMVEC, similarly to human cerebral microvascular endothelial cells (Kim et al., 2004; Li et al., 1999), rat brain capillary endothelial cells (Bartha et al., 2000; Brown et al., 2008), bovine pulmonary artery endothelial cells (Lum et al., 1992), human umbilical vein endothelial cells (HUVEC) and HUVEC-derived cell line ECV304 (Sandoval et al., 2001), thrombin increased  $[\text{Ca}^{2+}]_i$ . The magnitude of the  $\text{Ca}^{2+}$  response produced by thrombin in RBMVEC was dose-dependent. Treatment with the PAR1 antagonist, FR-171113 abolished the thrombin-induced  $\text{Ca}^{2+}$  response, indicating a critical role of PAR1 in this response. In endothelial cells, an increase in  $[\text{Ca}^{2+}]_i$  may be produced by  $\text{Ca}^{2+}$  influx and/or  $\text{Ca}^{2+}$  release from internal stores (Moccia et al., 2012). In the absence of extracellular  $\text{Ca}^{2+}$ , the response

to thrombin was slightly reduced indicating the participation of  $\text{Ca}^{2+}$  influx in this response, as previously reported (Bartha et al., 2000; Sandoval et al., 2001). However, the fast and transient nature of the increase in  $[\text{Ca}^{2+}]_i$  produced by thrombin was suggestive of  $\text{Ca}^{2+}$  release from internal stores (Moccia et al., 2012).

We next explored the internal  $\text{Ca}^{2+}$  stores involved in the response to thrombin. Blockade of ryanodine receptors reduced, and that of inositol 1,4,5-trisphosphate ( $\text{IP}_3$ ) receptors abolished the response to thrombin, indicating that thrombin promoted the  $\text{Ca}^{2+}$  release from endoplasmic reticulum, mainly via  $\text{IP}_3$  receptors. On the other hand, inhibition of lysosomal ATPase did not affect the response, indicating that the endolysosomal  $\text{Ca}^{2+}$  stores are not involved in the response to thrombin. These results support the  $\text{IP}_3$ -mediated  $\text{Ca}^{2+}$  release as the main mechanism of increase in  $[\text{Ca}^{2+}]_i$  by thrombin and a  $\text{G}_{q/11}$  coupling mechanism of thrombin-PAR1 in RBMVEC. Activation of phospholipase C downstream to  $\text{G}_q$  protein pathway cleaves the membrane phospholipid phosphatidylinositol-4,5-bisphosphate ( $\text{PIP}_2$ ) to the second messengers inositol-1,4,5-trisphosphate ( $\text{IP}_3$ ) and diacylglycerol (DAG) (Berridge, 2009). Previous reports indicate an increase in  $\text{IP}_3$  within 10–15 seconds after stimulation with thrombin in bovine pulmonary artery endothelial cells (Lum et al., 1992) or HUVEC (Sandoval et al., 2001).  $\text{IP}_3$ , acting on  $\text{IP}_3$  receptors, releases  $\text{Ca}^{2+}$  from endoplasmic reticulum. The local increase in  $\text{Ca}^{2+}$  further promotes  $\text{Ca}^{2+}$  release through ryanodine receptors, via  $\text{Ca}^{2+}$ -induced  $\text{Ca}^{2+}$  release mechanism. The fact that thrombin-induced increase in  $[\text{Ca}^{2+}]_i$  was reduced by blockade of ryanodine receptors, indicates that  $\text{Ca}^{2+}$  release from endoplasmic reticulum via ryanodine receptors, in addition to  $\text{IP}_3$  receptors, is involved in the response to thrombin in RBMVEC. In endothelial cells, similarly with other cells,  $\text{Ca}^{2+}$  release from ER and the consequent depletion of the ER store leads to  $\text{Ca}^{2+}$  influx via store-operated  $\text{Ca}^{2+}$  entry (SOCE) (Putney, 1986; Tiruppathi et al., 2006). Our results indicate that in RBMVEC thrombin releases  $\text{Ca}^{2+}$  from ER store and promotes  $\text{Ca}^{2+}$  influx via SOCE (Fig. 7). We recently reported that SOCE is a functional mechanism of  $\text{Ca}^{2+}$  entry in RBMVEC (Brailoiu et al., 2016). Similarly, thrombin elicited SOCE in HUVEC (Sandoval et al., 2001) or in mouse lung microvascular endothelial cells (Tiruppathi et al., 2002).

We next investigated  $\text{Ca}^{2+}$ -dependent pathways downstream of thrombin-PAR1 interaction in RBMVEC. An increase in NO production can occur via  $\text{Ca}^{2+}$ -dependent activation of NO synthase (Fleming et al., 1997). Using a NO-sensitive fluorescent dye, we identified that thrombin increased NO in RBMVEC; the effect was abolished by the inhibition of PAR1 or of NO synthase. Similarly, thrombin induced a transient  $[\text{Ca}^{2+}]_i$  increase and NO production in pig coronary artery endothelial cells (Mizuno et al., 1998). In pulmonary endothelial cells, thrombin had a biphasic effect: the acute thrombin stimulation stimulated eNOS, while prolonged treatment inhibited the NO production (Nickel et al., 2013). In addition to its critical roles in vascular tone (Bohlen, 2015; Furchgott and Vanhoutte, 1989), NO modulates permeability of different microvascular beds, including the blood-brain barrier (Kubes and Granger, 1992; Thiel and Audus, 2001). Compounds like sodium nitroprusside, that spontaneously generate NO, increased the permeability of the blood-brain barrier in rats (Shukla et al., 1996).



A local increase in cytosolic  $\text{Ca}^{2+}$  concentration,  $[\text{Ca}^{2+}]_i$ , is buffered by mitochondrial  $\text{Ca}^{2+}$  uptake (De Stefani et al., 2016). Previous reports indicate that  $\text{IP}_3$ -mediated increase in  $[\text{Ca}^{2+}]_i$  may be transmitted to the mitochondria, increasing mitochondrial  $\text{Ca}^{2+}$  and bioenergetics (Hajnóczky et al., 1995). Intramitochondrial  $\text{Ca}^{2+}$  activates mitochondrion-derived superoxide (mROS) production (Camello-Almaraz et al., 2006; Castilho et al., 1998). Our results indicate that in RBMVEC thrombin increased mROS production via PAR1 activation. In murine and pulmonary pulmonary vein endothelial cells, thrombin-evoked cytosolic  $\text{Ca}^{2+}$  mobilization was also followed by mROS increase (Hawkins et al., 2007).

Generation of reactive oxygen species (ROS) has been involved in endothelial dysfunction (Craige et al., 2015). To investigate this pathway, we assessed the effect of thrombin on cytosolic ROS, monitored with a ROS-sensitive fluorescent dye (Deliu et al., 2012). We found that thrombin increased cytosolic ROS formation. Likewise, thrombin was found to generate ROS in platelets (Carrim et al., 2015). However, in platelets, thrombin exerted its effect via a PAR4-dependent mechanism, while our results support a PAR1-dependent mechanism in RBMVEC. On the other hand, in hepatocellular carcinoma cells, thrombin induced ROS via both PAR1 and PAR4 (Mussbach et al., 2015). In endothelial cells from a mouse model of Alzheimer's disease, a direct thrombin inhibitor blocked ROS generation induced by hypoxia (Tripathy et al., 2013). To our knowledge, this is the first time when thrombin was shown to increase NO and ROS in RBMVEC.

In endothelial cells, similar to muscle cells, an increase in  $[\text{Ca}^{2+}]_i$  leads to activation of  $\text{Ca}^{2+}$ /calmodulin-dependent myosin light chain (MLC) kinase (MLCK), actin-myosin interaction, and cell retraction (Wysolmerski and Lagunoff, 1990) leading to increased permeability (De Bock et al., 2013). We examined the morphological changes induced by thrombin on the cytoskeleton and the tight junctions in RBMVEC. Thrombin increased F-actin stress fibers, reduced the peripheral ZO-1 staining, and induced gap formation, indicating cytoskeletal changes and disruption of tight junctions, and promoted an increase in permeability. These changes, consistent with barrier disruption, were similar to those reported in human or bovine pulmonary artery endothelial cells (Arce et al., 2008; Lum et al., 1992) or in mouse brain endothelial (bEnd.3) cells (Hun Lee et al., 2015). Also, in pulmonary microvascular endothelial cells, thrombin was shown to increase the permeability and alter the barrier function by F-actin cytoskeleton rearrangement (Birukova et al., 2009; Wang et al., 2015). Taken together, our results indicate multiple mechanisms by which thrombin modulate the activity of rat brain microvascular endothelial cells and may disrupt the blood-brain barrier function, with implications for pathological conditions such as stroke, brain trauma and inflammation.

## 4. Experimental Procedures

### 4.1. Chemicals and reagents

Thrombin from human plasma and FR-171113 (PAR1 antagonist) were from Sigma-Aldrich (St. Louis, MO). Bafilomycin A1 and xestospongin C were from Tocris Biosciences (Bristol, UK). Fura-2AM, DAF-FM diacetate, DiBAC<sub>4</sub>(3), CM-H<sub>2</sub>-DCFDA, MitoSOX Red, and

ActinRed555 were from Molecular Probes (ThermoFisher Scientific, Waltham, MA). Other reagents were from Sigma-Aldrich (St. Louis, MO) unless otherwise mentioned.

## 4.2. Cell Culture

Rat brain microvascular endothelial cells (RBMVEC) from Cell Applications, Inc (San Diego, CA) were cultured in rat brain endothelial basal medium and endothelial growth supplements, according to the manufacturer's instructions (Cell Applications, Inc), as previously described (Altmann et al., 2015; Brailoiu et al., 2016). Cells were grown in T75 flasks coated with attachment factor (Cell Applications, Inc) until 80% confluent. Cells were plated on round coverslips of 12 mm diameter (immunocytochemistry studies), or 25 mm diameter (live imaging studies), coated with human fibronectin (Discovery Labware, Bedford, MA).

## 4.3. Cytosolic $\text{Ca}^{2+}$ measurement

Measurements of intracellular  $\text{Ca}^{2+}$  concentration,  $[\text{Ca}^{2+}]_i$ , were performed as previously described (Altmann et al., 2015; Brailoiu et al., 2016). Briefly, cells were incubated with 5  $\mu\text{M}$  Fura-2 AM (Molecular Probes, ThermoFisher Scientific, Waltham, MA) in Hanks Balanced Salt Solution (HBSS) at room temperature for one hour and washed with dye-free HBSS. Coverslips were mounted in an open bath chamber (QR-40LP, Warner Instruments, Hamden, CT) on the stage of an inverted microscope Nikon Eclipse TiE (Nikon Inc., Melville, NY), equipped with a Perfect Focus System and a Photometrics CoolSnap HQ2 CCD camera (Photometrics, Tucson, AZ). During the experiments, the Perfect Focus System was activated. Fura-2 AM fluorescence (emission 510 nm), following alternate excitation at 340 and 380 nm, was acquired at a frequency of 0.25 Hz. Images were acquired/analyzed using NIS-Elements AR software (Nikon). After appropriate calibration, the ratio of the fluorescence signals (340/380 nm) was converted to  $\text{Ca}^{2+}$  concentrations (Grynkiewicz et al., 1985).

## 4.4. NO measurement

Intracellular NO was monitored with DAF-FM [(4-amino-5-methylamino-2',7'-difluoro-fluorescein) diacetate] (Molecular Probes) as previously described (Altmann et al., 2015; Kojima et al., 1998). RBMVEC were incubated at room temperature for 45 min in HBSS containing a DAF-FM (0.5  $\mu\text{M}$ ) this condition significantly reduced the background autofluorescence and improved the signal-to-noise ratio of NO detection in single cells (Leikert et al., 2001). After loading, cells were rinsed three times with saline. DAF-FM fluorescence ratio was measured using excitation and emission wavelengths of 488 nm and 540 nm, respectively, at a frequency of 0.1 Hz.

## 4.5. Detection of mitochondrial ROS accumulation

Measurement of mitochondrial ROS levels was carried out using the MitoSOX Red superoxide indicator (Molecular Probes), a novel and highly selective fluorogenic dye, as previously reported (Deliu et al., 2012). MitoSOX Red reagent permeates live cells, and rapidly and selectively targets mitochondria. At the mitochondrial level, it is rapidly oxidized by superoxide; oxidation of MitoSOX reagent leads to red fluorescence. Cells were



incubated with 3  $\mu$ M MitoSOX Red in HBSS at room temperature for 25 min in the dark, and washed with dye-free HBSS. The intensity of red fluorescence after excitation at 510 nm was acquired at a frequency of 0.25 Hz and evaluated as a measure of mitochondrial superoxide accumulation.

#### 4.6. Detection of cytosolic ROS accumulation

Assessment of cytosolic ROS levels was achieved using CM-H<sub>2</sub>-DCFDA [5-6-chloromethyl-27-dichlorodihydrofluorescein diacetate, acetyl ester] (Molecular Probes), as previously reported (Deliu et al., 2012). This assay is based on the principle that CMH<sub>2</sub>-DCFDA passively diffuses into cells; its acetate groups are cleaved by intracellular esterases and its thiol-reactive chloromethyl group reacts with intracellular glutathione and other thiols. In the presence of ROS, CM-H<sub>2</sub>-DCFDA is rapidly oxidized to become highly fluorescent product that is trapped inside the cell. Cells were incubated with 1  $\mu$ M CM-H<sub>2</sub>-DCFDA in HBSS at room temperature for 15 min, in the dark and washed with dye-free HBSS. The intensity of green fluorescence following excitation at 495 nm was acquired at a frequency of 0.25 Hz and evaluated as a measure of cytosolic ROS accumulation.

#### 4.7. Immunocytochemistry

Immunocytochemistry studies were carried out as previously described (Brailoiu et al., 2011). RBMVEC grown on coverslips until confluence, were treated with thrombin (0.5 u/ml) alone, or thrombin (0.5 u/ml) and FR-171113 (1  $\mu$ M); untreated cells served as control. The cells were rinsed in PBS, fixed in 4% paraformaldehyde, washed with PBS and PBS with 0.5% Triton X for 5 min, blocked with normal goat serum, then incubated with primary antibody ZO-1 (rabbit IgG, Molecular Probes) overnight at 4°C. After washing in PBS, the cells were incubated with secondary antibody conjugated to Alexa 488 goat anti-rabbit, 2 hours at room temperature. After further washing with PBS, the cells were incubated for 30 min with ActinRed 555 (Molecular Probes), then washed in PBS, mounted with DAPI Fluoromount G (SouthernBiotech, Birmingham, AL) and sealed. The cells were examined under a Leica DMI6000B fluorescence microscope equipped with the appropriate excitation/emission filters.

#### 4.7 Permeability assay

RBMVEC were cultured in cell culture inserts with transparent PET membrane, 1  $\mu$ m pore size (Corning/Falcon, Thomas Scientific) coated with human fibronectin, in 24 well plates, at a density of  $3.5 \times 10^4$  cells/ insert, similarly with previous reports (Monaghan-Benson and Wittchen, 2011). Cells were grown until they reached confluence (2–3 days). In the day of the experiment, the growth medium was removed from the cell insert and replaced with medium containing Fluorescein isothiocyanate (FITC)-dextran 40,000 KDa (control) or the drug dissolved in medium containing FITC-dextran (treatment). FITC-dextran, 1mg/ml (Sigma-Aldrich) was freshly prepared just before the experiment. To quantify the passage of FITC-dextran across the cell monolayer, 50  $\mu$ l of medium was removed from the bottom of the well and transferred to a 96-well plate at the time of treatment (0 min) and after 15, 30, 45, 60 and 120 mins. The FITC intensity (excitation 480 nm, emission 520 nm) was measured using a Synergy 2 (Biotek Instruments Inc, Winooski, Vermont) plate reader. Experiments were carried out in triplicates.

#### 4.8. Statistical analysis

Data were expressed as mean  $\pm$  standard error of mean (SEM). One-way ANOVA followed by post hoc analysis using Bonferonni and Tukey tests was used to evaluate significant differences between groups;  $P < 0.05$  was considered statistically significant.

#### Acknowledgments

This study was supported by startup funds from the Jefferson College of Pharmacy, and by the National Institutes of Health (grants R01 DA035926 and P30 DA 013429).

#### Abbreviations

<b>BBB</b>	blood-brain barrier
<b>[Ca<sup>2+</sup>]<sub>i</sub></b>	cytosolic Ca <sup>2+</sup> concentration
<b>IP<sub>3</sub></b>	inositol 1,4,5-trisphosphate
<b>L-NAME</b>	NG-nitro-L-arginine methyl ester
<b>NO</b>	nitric oxide
<b>PAR1</b>	protease-activated receptor 1
<b>RBMVEC</b>	rat brain microvascular endothelial cells
<b>u</b>	units

#### References

- Abbott NJ, Patabendige AA, Dolman DE, Yusof SR, Begley DJ. Structure and function of the blood-brain barrier. *Neurobiol Dis.* 2010; 37:13–25. [PubMed: 19664713]
- Alexander SP, Davenport AP, Kelly E, Marrion N, Peters JA, Benson HE, Faccenda E, Pawson AJ, Sharman JL, Southan C, Davies JA, Collaborators C. The Concise Guide to PHARMACOLOGY 2015/16: G protein-coupled receptors. *Br J Pharmacol.* 2015; 172:5744–869. [PubMed: 26650439]
- Altmann JB, Yan G, Meeks JF, Aboud ME, Brailoiu E, Brailoiu GC. G protein-coupled estrogen receptor-mediated effects on cytosolic calcium and nanomechanics in brain microvascular endothelial cells. *J Neurochem.* 2015; 133:629–39. [PubMed: 25703621]
- Arce FT, Whitlock JL, Birukova AA, Birukov KG, Arnsdorf MF, Lal R, Garcia JG, Dudek SM. Regulation of the micromechanical properties of pulmonary endothelium by S1P and thrombin: role of cortactin. *Biophys J.* 2008; 95:886–94. [PubMed: 18408039]
- Bartha K, Domotor E, Lanza F, Adam-Vizi V, Machovich R. Identification of thrombin receptors in rat brain capillary endothelial cells. *J Cereb Blood Flow Metab.* 2000; 20:175–82. [PubMed: 10616806]
- Berridge MJ. Inositol trisphosphate and calcium signalling mechanisms. *Biochim Biophys Acta.* 2009; 1793:933–40. [PubMed: 19010359]
- Birukova AA, Arce FT, Moldobaeva N, Dudek SM, Garcia JG, Lal R, Birukov KG. Endothelial permeability is controlled by spatially defined cytoskeletal mechanics: atomic force microscopy force mapping of pulmonary endothelial monolayer. *Nanomedicine.* 2009; 5:30–41. [PubMed: 18824415]
- Bohlen HG. Nitric oxide and the cardiovascular system. *Compr Physiol.* 2015; 5:808–23. [PubMed: 25880514]

- Bowman EJ, Siebers A, Altendorf K. Bafilomycins: a class of inhibitors of membrane ATPases from microorganisms, animal cells, and plant cells. *Proc Natl Acad Sci U S A*. 1988; 85:7972–6. [PubMed: 2973058]
- Brailoiu GC, Oprea TI, Zhao P, Abood ME, Brailoiu E. Intracellular cannabinoid type 1 (CB1) receptors are activated by anandamide. *J Biol Chem*. 2011; 286:29166–74. [PubMed: 21719698]
- Brailoiu GC, Deliu E, Console-Bram LM, Soboloff J, Abood ME, Unterwald EM, Brailoiu E. Cocaine inhibits store-operated  $\text{Ca}^{2+}$  entry in brain microvascular endothelial cells: critical role for sigma-1 receptors. *Biochem J*. 2016; 473:1–5. [PubMed: 26467159]
- Brown RC, Wu L, Hicks K, O'Neil RG. Regulation of blood-brain barrier permeability by transient receptor potential type C and type v calcium-permeable channels. *Microcirculation*. 2008; 15:359–71. [PubMed: 18464164]
- Camello-Almaraz C, Gomez-Pinilla PJ, Pozo MJ, Camello PJ. Mitochondrial reactive oxygen species and  $\text{Ca}^{2+}$  signaling. *Am J Physiol Cell Physiol*. 2006; 291:C1082–8. [PubMed: 16760264]
- Cardoso FL, Brites D, Brito MA. Looking at the blood-brain barrier: molecular anatomy and possible investigation approaches. *Brain Res Rev*. 2010; 64:328–63. [PubMed: 20685221]
- Carrim N, Arthur JF, Hamilton JR, Gardiner EE, Andrews RK, Moran N, Berndt MC, Metharom P. Thrombin-induced reactive oxygen species generation in platelets: A novel role for protease-activated receptor 4 and GPIIb/IIIa. *Redox Biol*. 2015; 6:640–7. [PubMed: 26569550]
- Castilho RF, Hansson O, Ward MW, Budd SL, Nicholls DG. Mitochondrial control of acute glutamate excitotoxicity in cultured cerebellar granule cells. *J Neurosci*. 1998; 18:10277–86. [PubMed: 9852565]
- Cirino G, Napoli C, Bucci M, Cicala C. Inflammation-coagulation network: are serine protease receptors the knot? *Trends Pharmacol Sci*. 2000; 21:170–2. [PubMed: 10785649]
- Craige SM, Kant S, Keaney JF Jr. Reactive oxygen species in endothelial function - from disease to adaptation. *Circ J*. 2015; 79:1145–55. [PubMed: 25986771]
- De Bock M, Wang N, Decrock E, Bol M, Gadicherla AK, Culot M, Cecchelli R, Bultynck G, Leybaert L. Endothelial calcium dynamics, connexin channels and blood-brain barrier function. *Prog Neurobiol*. 2013; 108:1–20. [PubMed: 23851106]
- De Stefani D, Rizzuto R, Pozzan T. Enjoy the Trip: Calcium in Mitochondria Back and Forth. *Annu Rev Biochem*. 2016; 85:161–92. [PubMed: 27145841]
- Deliu E, Brailoiu GC, Arterburn JB, Oprea TI, Benamar K, Dun NJ, Brailoiu E. Mechanisms of G protein-coupled estrogen receptor-mediated spinal nociception. *J Pain*. 2012; 13:742–54. [PubMed: 22858342]
- Fleming I, Bauersachs J, Busse R. Calcium-dependent and calmodulin-dependent activation of the endothelial NO synthase. *J Vasc Res*. 1997; 34:165–74. [PubMed: 9226298]
- Furchgott RF, Vanhoutte PM. Endothelium-derived relaxing and contracting factors. *FASEB J*. 1989; 3:2007–18. [PubMed: 2545495]
- Gingrich MB, Traynelis SF. Serine proteases and brain damage - is there a link? *Trends Neurosci*. 2000; 23:399–407. [PubMed: 10941185]
- Grynkiewicz G, Poenie M, Tsien RY. A new generation of  $\text{Ca}^{2+}$  indicators with greatly improved fluorescence properties. *J Biol Chem*. 1985; 260:3440–50. [PubMed: 3838314]
- Hajnóczky G, Robb-Gaspers LD, Seitz MB, Thomas AP. Decoding of cytosolic calcium oscillations in the mitochondria. *Cell*. 1995; 82:415–24. [PubMed: 7634331]
- Hawkins BJ, Solt LA, Chowdhury I, Kazi AS, Abid MR, Aird WC, May MJ, Foscett JK, Madesh M. G protein-coupled receptor  $\text{Ca}^{2+}$ -linked mitochondrial reactive oxygen species are essential for endothelial/leukocyte adherence. *Mol Cell Biol*. 2007; 27:7582–93. [PubMed: 17724077]
- Hawkins BT, Gu YH, Izawa Y, Del Zoppo GJ. Dabigatran abrogates brain endothelial cell permeability in response to thrombin. *J Cereb Blood Flow Metab*. 2015
- Hollenberg MD, Compton SJ. International Union of Pharmacology. XXVIII. Proteinase-activated receptors. *Pharmacol Rev*. 2002; 54:203–17. [PubMed: 12037136]
- Hun Lee J, Won S, Stein DG. Progesterone attenuates thrombin-induced endothelial barrier disruption in the brain endothelial cell line bEnd.3: The role of tight junction proteins and the endothelial protein C receptor. *Brain Res*. 2015; 1613:73–80. [PubMed: 25862570]

- Kim YV, Di Cello F, Hillaire CS, Kim KS. Differential Ca<sup>2+</sup> signaling by thrombin and protease-activated receptor-1-activating peptide in human brain microvascular endothelial cells. *Am J Physiol Cell Physiol*. 2004; 286:C31–42. [PubMed: 12944324]
- Kojima H, Nakatsubo N, Kikuchi K, Kawahara S, Kirino Y, Nagoshi H, Hirata Y, Nagano T. Detection and imaging of nitric oxide with novel fluorescent indicators: diaminofluoresceins. *Anal Chem*. 1998; 70:2446–53. [PubMed: 9666719]
- Kubes P, Granger DN. Nitric oxide modulates microvascular permeability. *Am J Physiol*. 1992; 262:H611–5. [PubMed: 1539722]
- Kuhlmann CR, Gerigk M, Bender B, Closhen D, Lessmann V, Luhmann HJ. Fluvastatin prevents glutamate-induced blood-brain-barrier disruption in vitro. *Life Sci*. 2008; 82:1281–7. [PubMed: 18534629]
- Leikert JF, Rathel TR, Muller C, Vollmar AM, Dirsch VM. Reliable in vitro measurement of nitric oxide released from endothelial cells using low concentrations of the fluorescent probe 4,5-diaminofluorescein. *FEBS Lett*. 2001; 506:131–4. [PubMed: 11591386]
- Li L, Bressler B, Prameya R, Dorovini-Zis K, Van Breemen C. Agonist-stimulated calcium entry in primary cultures of human cerebral microvascular endothelial cells. *Microvasc Res*. 1999; 57:211–26. [PubMed: 10329249]
- Lum H, Aschner JL, Phillips PG, Fletcher PW, Malik AB. Time course of thrombin-induced increase in endothelial permeability: relationship to Ca<sup>2+</sup> and inositol polyphosphates. *Am J Physiol*. 1992; 263:L219–25. [PubMed: 1514647]
- Mizuno O, Hirano K, Nishimura J, Kubo C, Kanaide H. Mechanism of endothelium-dependent relaxation induced by thrombin in the pig coronary artery. *Eur J Pharmacol*. 1998; 351:67–77. [PubMed: 9698207]
- Moccia F, Berra-Romani R, Tanzi F. Update on vascular endothelial Ca(2+) signalling: A tale of ion channels, pumps and transporters. *World J Biol Chem*. 2012; 3:127–58. [PubMed: 22905291]
- Monaghan-Benson E, Wittchen ES. In vitro analyses of endothelial cell permeability. *Methods Mol Biol*. 2011; 763:281–90. [PubMed: 21874459]
- Mussbach F, Henklein P, Westermann M, Settmacher U, Bohmer FD, Kaufmann R. Proteinase-activated receptor 1- and 4-promoted migration of Hep3B hepatocellular carcinoma cells depends on ROS formation and RTK transactivation. *J Cancer Res Clin Oncol*. 2015; 141:813–25. [PubMed: 25373316]
- Nickel KF, Laux V, Heumann R, von Degenfeld G. Thrombin has biphasic effects on the nitric oxide-cGMP pathway in endothelial cells and contributes to experimental pulmonary hypertension. *PLoS One*. 2013; 8:e63504. [PubMed: 23785394]
- Putney JW Jr. A model for receptor-regulated calcium entry. *Cell Calcium*. 1986; 7:1–12. [PubMed: 2420465]
- Rasmussen UB, Vouret-Craviari V, Jallat S, Schlesinger Y, Pages G, Pavirani A, Lecocq JP, Pouyssegur J, Van Obberghen-Schilling E. cDNA cloning and expression of a hamster alpha-thrombin receptor coupled to Ca<sup>2+</sup> mobilization. *FEBS Lett*. 1991; 288:123–8. [PubMed: 1652467]
- Sandoval R, Malik AB, Naqvi T, Mehta D, Tiruppathi C. Requirement for Ca<sup>2+</sup> signaling in the mechanism of thrombin-induced increase in endothelial permeability. *Am J Physiol Lung Cell Mol Physiol*. 2001; 280:L239–47. [PubMed: 11159002]
- Shukla A, Dikshit M, Srimal RC. Nitric oxide-dependent blood-brain barrier permeability alteration in the rat brain. *Experientia*. 1996; 52:136–40. [PubMed: 8608814]
- Siller-Matula JM, Schwameis M, Blann A, Mannhalter C, Jilma B. Thrombin as a multi-functional enzyme. Focus on in vitro and in vivo effects. *Thromb Haemost*. 2011; 106:1020–33. [PubMed: 21979864]
- Thiel VE, Audus KL. Nitric oxide and blood-brain barrier integrity. *Antioxid Redox Signal*. 2001; 3:273–8. [PubMed: 11396481]
- Tiruppathi C, Minshall RD, Paria BC, Vogel SM, Malik AB. Role of Ca<sup>2+</sup> signaling in the regulation of endothelial permeability. *Vascul Pharmacol*. 2002; 39:173–85. [PubMed: 12747958]
- Tiruppathi C, Ahmmed GU, Vogel SM, Malik AB. Ca<sup>2+</sup> signaling, TRP channels, and endothelial permeability. *Microcirculation*. 2006; 13:693–708. [PubMed: 17085428]

- Tripathy D, Sanchez A, Yin X, Luo J, Martinez J, Grammas P. Thrombin, a mediator of cerebrovascular inflammation in AD and hypoxia. *Front Aging Neurosci.* 2013; 5:19. [PubMed: 23675346]
- Vajda S, Bartha K, Wilhelm I, Krizbai IA, Adam-Vizi V. Identification of protease-activated receptor-4 (PAR-4) in puromycin-purified brain capillary endothelial cells cultured on Matrigel. *Neurochem Int.* 2008; 52:1234–9. [PubMed: 18294734]
- Vu TK, Hung DT, Wheaton VI, Coughlin SR. Molecular cloning of a functional thrombin receptor reveals a novel proteolytic mechanism of receptor activation. *Cell.* 1991; 64:1057–68. [PubMed: 1672265]
- Wang J, Li C, Chen T, Fang Y, Shi X, Pang T, Zhang L, Liao H. Nafamostat mesilate protects against acute cerebral ischemia via blood-brain barrier protection. *Neuropharmacology.* 2016; 105:398–410. [PubMed: 26861077]
- Wang X, Bleher R, Brown ME, Garcia JG, Dudek SM, Shekhawat GS, Dravid VP. Nano-Biomechanical Study of Spatio-Temporal Cytoskeleton Rearrangements that Determine Subcellular Mechanical Properties and Endothelial Permeability. *Sci Rep.* 2015; 5:11097. [PubMed: 26086333]
- Wysolmerski RB, Lagunoff D. Involvement of myosin light-chain kinase in endothelial cell retraction. *Proc Natl Acad Sci U S A.* 1990; 87:16–20. [PubMed: 2296576]
- Yin X, Wright J, Wall T, Grammas P. Brain endothelial cells synthesize neurotoxic thrombin in Alzheimer's disease. *Am J Pathol.* 2010; 176:1600–6. [PubMed: 20150433]

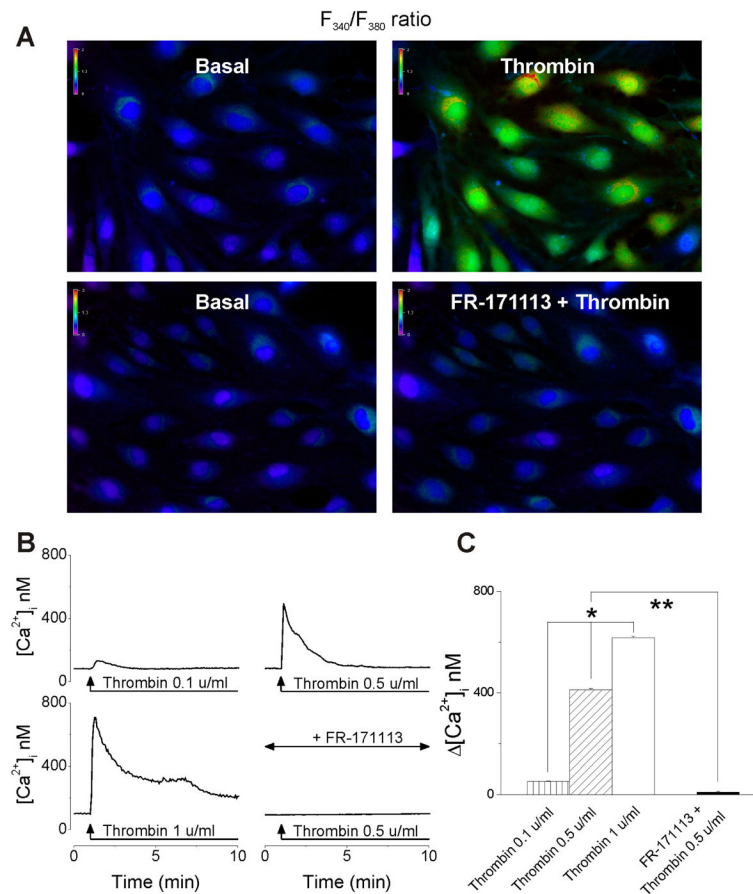


**Figure 1. Thrombin increases cytosolic Ca<sup>2+</sup> concentration, [Ca<sup>2+</sup>]<sub>i</sub>, in RBMVEC**

**A**, Examples of fura-2 AM fluorescence ratio ( $F_{340}/F_{380}$ ) in RBMVEC before (basal) and after treatment with thrombin (0.5 u/ml), or thrombin (0.5 u/ml) in cells pretreated with the PAR-1 antagonist, FR-171113 (1  $\mu$ M). Cold colors represent low ratios and hot colors represent high ratio (scale 0–2). **B**, Representative examples of [Ca<sup>2+</sup>]<sub>i</sub> increases produced by thrombin (0.1 u/ml, 0.5 u/ml and 1 u/ml) and thrombin (0.5 u/ml) in the presence of FR-171113 (1  $\mu$ M). Thrombin induced a fast and transient increase in [Ca<sup>2+</sup>]<sub>i</sub> whose amplitude was dose-dependent; the response to thrombin was abolished by FR-171113. **C**, Comparison of the amplitude of [Ca<sup>2+</sup>]<sub>i</sub> produced by each concentration of thrombin tested and by thrombin (0.5 u/ml) in the presence of FR-171113 (1  $\mu$ M).  $P < 0.05$  as compared to the response to the other concentrations of thrombin tested (\*), or to the response produced by thrombin 0.5 u/ml (\*\*).



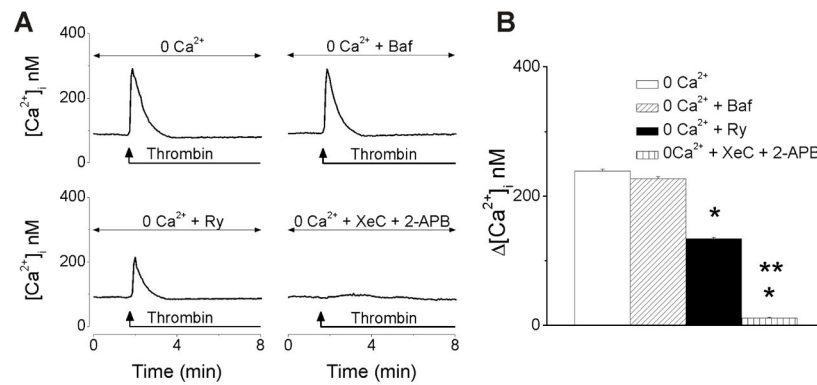


**Figure 2. Thrombin releases  $Ca^{2+}$  from endoplasmic reticulum**

**A**, Examples of increases in  $[Ca^{2+}]_i$  produced by thrombin in  $Ca^{2+}$ -free HBSS, in the absence and presence of inhibitors of lysosomal and endoplasmic reticulum  $Ca^{2+}$  stores. Disruption of lysosomal  $Ca^{2+}$  stores with bafilomycin A1 (Baf, 1  $\mu$ M, 1 h), did not affect the response to thrombin. Inhibition of ryanodine receptors with ryanodine (Ry, 1  $\mu$ M, 1 h) reduced the response to thrombin, and blockade of  $IP_3$  receptors with xestospongin C (XeC, 10  $\mu$ M, 15 min) and 2-APB (100  $\mu$ M, 15 min) abolished the response to thrombin. **B**, Comparison of the amplitude of  $Ca^{2+}$  responses produced by thrombin in each of the conditions mentioned.  $P < 0.05$  as compared to the response to thrombin in  $Ca^{2+}$ -free HBSS (\*), or in the presence of ryanodine (\*\*).

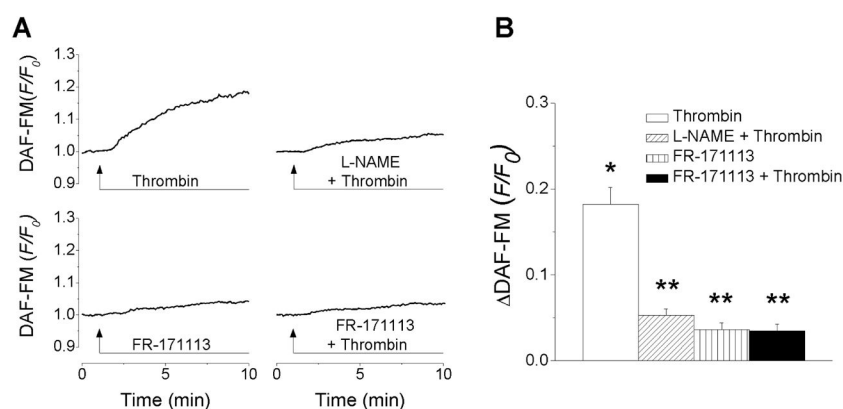


**Figure 3. Thrombin increases nitric oxide (NO) production in RBMVEC**

**A**, Examples of increases in DAF-FM diacetate fluorescence ratio ( $F/F_0$ ), as a measure of NO level, produced by thrombin (0.5 u/ml) in the absence and presence of L-NAME and of PAR-1 antagonist, FR-171113 (1  $\mu$ M). The effect of FR-171113 (1  $\mu$ M) alone is also illustrated. **B**, Comparison of increases in DAF-FM ratio in each of the conditions mentioned; L-NAME and FR-171113 abolished the response produced by thrombin.  $P < 0.05$  as compared to the basal level (\*), or to the response produced by thrombin (\*\*).

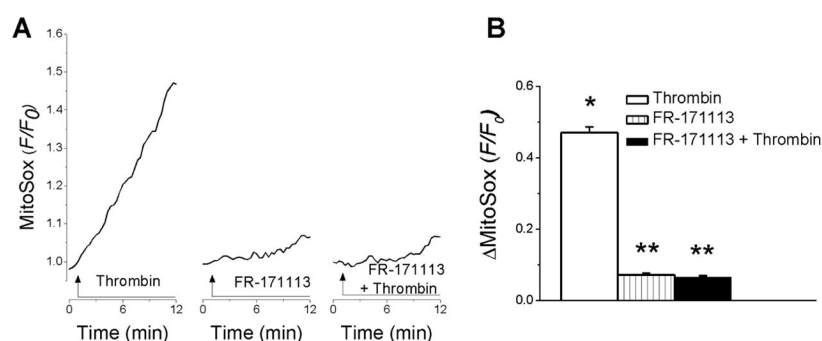


**Figure 4. Thrombin increases mitochondrial superoxide in RBMVEC**

**A**, Examples of increases in MitoSOX Red fluorescence ratio (F/F<sub>0</sub>), as a measure of mitochondrial superoxide produced by thrombin (0.5 u/ml) in the absence and presence of the PAR-1 antagonist, FR-171113 (1 μM) or by FR-171113 (1 μM) alone. **B**, Comparison of increases in MitoSOX Red fluorescence ratio produced by thrombin alone or in the presence of FR-171113. The PAR-1 antagonist abolished the response produced by thrombin.  $P < 0.05$  as compared to the response produced by thrombin (\*).  $P < 0.05$  as compared to the basal level (\*), or to the response produced by thrombin (\*\*).

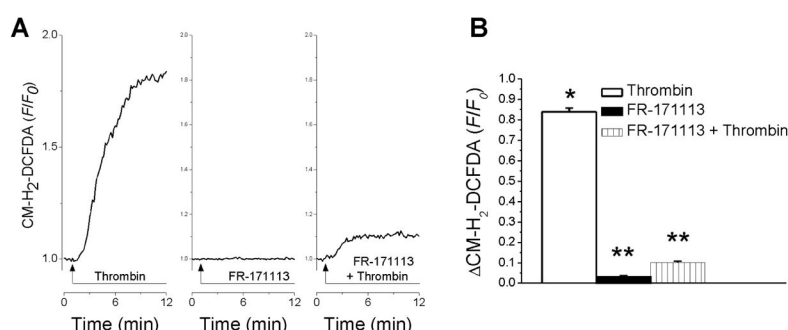


**Figure 5. Thrombin increases cytosolic ROS in RBMVEC**

**A**, Examples of increases in CM-D<sub>2</sub>-DCFDA fluorescence ratio (F/F<sub>0</sub>), as a measure of ROS level, produced by thrombin (0.5 u/ml), FR-171113 (1 μM) and thrombin in the presence of FR-171113 (1 μM). **B**, Comparison of increases in CM-D<sub>2</sub>-DCFDA ratio produced by thrombin alone, FR-171113 alone or thrombin in the presence of FR-171113. The PAR-1 antagonist while did not have a significant effect by itself, abolished the response produced by thrombin.  $P < 0.05$  as compared to the basal level (\*), or to the response produced by thrombin (\*\*).

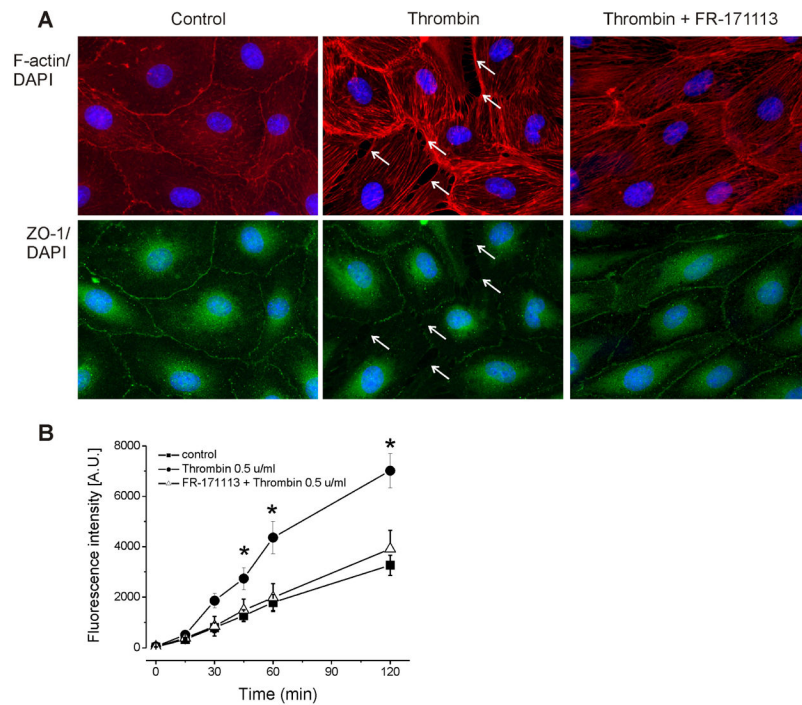


**Figure 6. Morphological changes induced by thrombin in RBMVEC**

**A**, Distribution of F-actin (red), a component of cytoskeleton, and ZO-1 (green), a component of tight junctions, in RBMVEC in control cells, cells treated with thrombin (0.5 u/ml) or thrombin (0.5 u/ml) and FR-171113 (1  $\mu$ M). Treatment with thrombin increased F-actin stress fiber formation, produced a reduction in ZO-1 staining, indicating cytoskeletal rearrangement and disruption of tight junctions; in addition, intercellular gaps, indicated by arrows, became visible in the endothelial monolayer. Pretreatment with the PAR1 antagonist prevented the changes produced by thrombin. Cellular nuclei were stained with DAPI. **B**, Thrombin increased the permeability of RBMVEC monolayers assessed using the FITC-dextran flux assay \* $P < 0.05$  as compared to control.

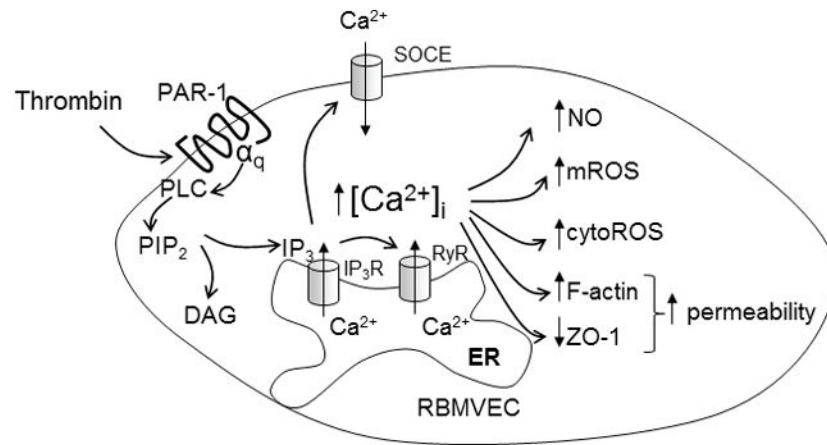


**Figure 7. Proposed mechanism of thrombin effects in RBMVEC**

Thrombin acting on PAR1, produces Ca<sup>2+</sup> release from endoplasmic reticulum (ER) via inositol 1,4,5-trisphosphate receptors (IP<sub>3</sub>) receptors, and ryanodine receptors (RyR). Depletion of ER Ca<sup>2+</sup> store leads to Ca<sup>2+</sup> influx (store-operated Ca<sup>2+</sup> entry, SOCE). The increase in [Ca<sup>2+</sup>]<sub>i</sub> promotes NO formation, increase mitochondrion-derived superoxide (mROS) and cytosolic ROS (cytoROS) levels and determines cytoskeletal changes (increase in F-actin stress fibers formation) and disruption of tight junctions, leading to increased permeability and barrier dysfunction. Abbreviations: PIP<sub>2</sub> phosphatidylinositol-4,5-bisphosphate; PLC, phospholipase C.